Carbon Science

Vol. 6, No. 2 June 2005 pp. 89-95

Porosity and Liquid-phase Adsorption Characteristics of Activated Carbons Prepared From Peach Stones by H_3PO_4

Amina A. Attia♠, Badie S. Girgis and Nady A. F. Tawfik

National Research Centre, 12622 Dokki, Cairo, Egypt.
♠e-mail: *nady_attia@yahoo.com*
(Received February 15, 2005; Accepted May 6, 2005)

Abstract

Crushed peach stone shells were impregnated with H_3PO_4 of increasing concentrations (30-70%) followed by heat treatment at 773 K for 3 h. Produced carbons (ACs) were characterized by N_2 adsorption at 77 K using the BET-equation and the α_s-method. High surface area microporous ACs were obtained, with enhanced internal pore volume, as function of % H_3PO_4. Adsorption isotherms from aqueous solution were determined for methylene blue (MB) and p-nitrophenol (PNP), as representatives for dye and phenolics pollutant molecules. Application of the Langmuir model proved the high limiting capacity towards both solute molecules, MB was uptaken in increasing amounts as function of H_3PO_4 concentration and generated porosity. High removal of PNP was almost the same irrespective of porosity characteristics. Competitive adsorption of H_2O molecules on the hydrophilic carbon surface seems to partially reduce the available area to the PNP molecules. Application of the pseudo-second order law described well the fast adsorption (≤ 120 min) at two initial dye concentrations.

Keywords : *Activated carbon, Adsorption capacity, Peach stones, H_3PO_4 activation, Kinetic removal*

1. Introduction

Environmental pollution has grown extensively in the last few decades, as a result of increased fluid discharges from industrial and agricultural processes. It became necessary to limit it, treat and get pure water and air by applying convenient treatment schemes. Activated (or porous) carbons emerged as one of the best available technologies (BAT) for purification, separation, and recovery in various sectors and processes. They are extremely versatile adsorbents and their important applications relate to their use in the removal of odour, colour, taste and other undesirable organic impurities from potable water. Moreover, they are used in the treatment of domestic and industrial wastewater, solvent recovery, air purification in inhabited areas such as restaurants, food-processing and chemical industry, for removal of colour from various types of sugar syrup, in air pollution control, in purification of many chemicals, pharmaceutical and food products and in a variety of gas phase applications. Along with other inorganics, these activated carbons are used as catalysts and catalyst-support [1].

Activated carbons owe their distinguished properties because of two characteristics: (a) an extended surface area, microporous structure, high adsorption capacity and high degree of surface reactivity, and (b) good physical properties such as, hardness, density and versatility (e.g. obtained in various forms: powdered, granular, pellets, spheres, fibres and extrudates). These properties depend essentially on both of the raw material and the processing conditions. Conventional carbon precursors are: wood, coal, lignite, coconut shell, peat and others [2]. Agricultural by-products present a very important source for carbonaceous feedstocks due to being abundant, renewable, low-ash and low-cost materials. To this effect, Heschel and Klose [3] displayed a wide menu for candidates from this group covering several woods, nut shells and fruit stones. They divided them in the order of their suitability for the production of activated carbon: excellent (coconut shells, peach stones), highly suitable (plum stones, hazelnut shells), and less suitable (walnut shells, cherry stones). Thus, peach stones were considered to belong to the group of excellent carbon precursors, and attributed this superiority as not due to material-specific features (elemental composition) but by type-specific features. Coconut shells and peach stones are characterized by high values of apparent and true densities with low inherent porosity (~14%) [3]. On the other hand, coarse-cellular structures (e.g. in woods), which is indicated by porosities of raw materials higher than ~35%, are disadvantageous. These findings were based on data derived from the conventional thermal activation route, primary pyrolysis at 750-950 °C followed by steam-activation at 750-950 °C, where the burnoff of the chars varied from 25 to 80 wt %.

Activation with H_3PO_4 appeared in the last few decades to offer better processing conditions in comparison to both the above-mentioned thermal activation scheme as well as the chemical route using zinc chloride [4-10]. Thus, it involves

only a single heat treatment step achieved at lower temperatures (400-600 °C), leads to higher carbon yields and most of the phosphoric acid can be recovered after the process is completed. Thus, it is a material-, energy-, and time-saving scheme for the production of activated carbons [9]. Its main variables are: the impregnant concentration (or impregnation ratio) and the heat treatment temperature (HTT). Keeping the precursor, HTT, duration of treatment and washing conditions constant, the amount of impregnant (H_3PO_4) incorporated during the impregnation stages becomes the essential parameter that determine the porosity of the obtained activated carbon. A temperature of 500 °C (HTT) was chosen as it was demonstrated to be the most favorable to achieve the best effect in case of plant- origin carbon precursors [5-13]. The present study intends to postulate the effect of varying H_3PO_4 concentrations on the texture and adsorption characteristics of activated carbon derived from peach stone (shells) thermally treated at a constant temperature of 500 °C. Porosity development was followed by determining the N_2/77 K adsorption isotherms and their subsequent analysis by the established procedures of BET, α_s-methods. Liquid-phase adsorption isotherms of two molecules, methylene blue (MB) and p-nitrophenol (PNP) were estimated as representative of pollution substances (dyes and phenol). Kinetic removal of MB was determined, as well, and several mathematical models were applied. The feasibility of this lignocellulosic by-product is demonstrated under the mentioned processing scheme.

2. Experimental

2.1. Activated carbons

Peach stones were obtained from the local Egyptian processing zone of peach fruits. The dried, depitted, stones were ground and sieved to get the fraction within the 0.5-3 mm range. The activating agent of choice was chemical grade ortho-phosphoric acid (85 wt %). Four activated carbons were prepared by impregnation with different concentrations of H_3PO_4 acid (30, 40, 50 and 70%), and left in contact with raw material for 24 h in a drying air oven at 80 °C. Next day, the semi-dry mass was introduced into an S.S. reactor and admitted into an electric tube furnace where it was pyrolyzed for 3 h at 500 °C. The resulting carbons were thoroughly washed with hot water up to pH ≈ 6.5, then dried at 110 °C till constant weight and kept in tightly closed containers.

2.2. Characterization of Activated Carbons

2.2.1. Evaluation of Texture Parameters

This was achieved by determination of the N_2/77 K adsorption isotherms using Gemini 2365, V3.03 Sorptometer, a product of Micromeritics. Porosity characteristics were derived by application of the BET and α_s-methods [14]. The equivalent specific surface area was calculated by applying the BET model in the range of $P/P^o = 0.02$-0.20, (S_{BET}), and the total pore volume from amount of nitrogen adsorbed at $P/P^o = 0.95$, (V_P). Several texture parameters were calculated from the α_s-method, where the adsorbed volume of nitrogen (Va, cm^3/g) was plotted against α_s-values reported by Sellez-Perez and Martin-Martinez [14]. Three porous characteristics are determined: total surface area (S^{α}_t), non-microporous surface area (S^{α}_n) and micropore volume (V^{α}_o). An estimate for the mesopore volume (V_{meso}) was calculated from $V_{meso} = V_P - V^{\alpha}_o$.

2.2.2. Liquid-phase Adsorption

Adsorption isotherms of two probe molecules, MB and PNP were determined from aqueous solutions at room temperature. From stock solutions of 1 g/L for both solutes, various concentrations of MB and PNP solutions ranging from 80-800 and 50-500 $mg \cdot dm^{-3}$, respectively, were prepared by dilution with distilled water. Weighed amounts of 100 mg of each carbon were transferred to dry glass 250 ml bottles with glass stoppers and 100 ml of either of the two solutes were poured, at the requisite initial concentrations. The stoppered bottles were agitated for 72 h, and the residual concentration was measured at maximum lengths for MB, $\lambda = 664$ nm, and PNP, $\lambda = 317$ nm, using UV/Vis- spectrophotometer, Shimadzu (UV-2401 PC) model.

The amount of dye adsorbed on the carbon, q_e (mg/g) was calculated by the mass balance relationship;

$$q_e = \frac{(C_o - C_e) \times V}{W} \quad (1)$$

where C_o and C_e are the initial and equilibrium liquid-phase concentrations (mg/L), respectively, V (in L) is the volume of substrate solution and W is the weight of carbon used in g [15]. The isotherm equilibrium data were analyzed by applying the Langmuir isotherm model in its linear form [16];

$$C_e/q_e = 1/K_L\ Q_o + C_e/Q_o \quad (2)$$

where Q_o (mg/g) is the maximum amount of adsorption corresponding to complete monolayer coverage on the surface, C_e is the adsorbate equilibrium concentration and K_L (L/mg) is the Langmuir constant. From slope and intercept of the linearized C_e/q_e vs. C_e plot, both model constants are obtained [16]. The Langmuir isotherm can also be represented in terms of a dimensionless constant separation factor, or an equilibrium parameter, R_L;

$$R_L = 1/(1 + K_L\ C_o) \quad (3)$$

where K_L is the Langmuir constant and C_o is the maximum initial concentration [16]. According to Rao *et al.* [17], R_L values between 0 and 1 indicate favourable adsorption, $R_L = 0$ reversible isotherm, $R_L = 1$ linear isotherm, and $R_L > 1$ unfavourable isotherm. The free energy of adsorption, ΔG^o can also be evaluated from the parameter K_L (mol/L) accord-

ing to the expression [16];

$$\Delta G^{o}_{ads} = - RT \ln K_L \quad (4)$$

3. Results and Discussion

3.1. Porous Properties of Prepared Activated Carbons

Figs. 1 and 2 display the N_2/77 K adsorption isotherms as well as the corresponding α_s-plots. The features of both plots strongly predict the prevalence of microporosity in the tested carbons. A type I, in the BDDT classification of N_2 isotherms, indicates an essentially microporous adsorbent with slight or no external surface area. In addition, according to the α_s-plots classification advanced by Sellez-Perez and Martin-Martinez [18], our present plots (Fig. 2) belong to the typical α1- a type. This type is distinguished by having only one linear straight portion parallel to the abscissa axis and starting at an α_s value near to 1. The evaluated porous parameters are given in Table 1.

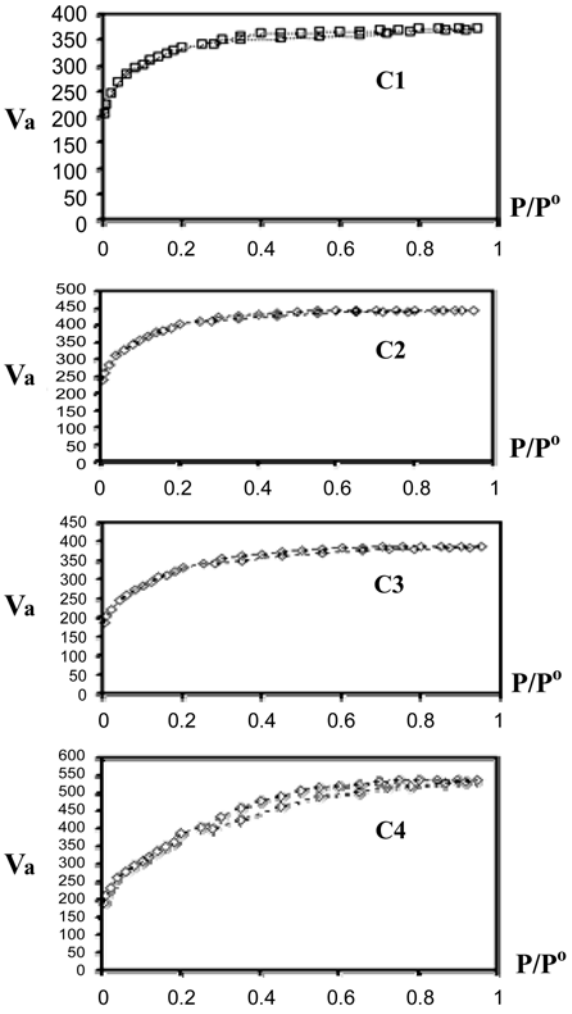

Fig. 1. Adsorption Isotherms of N_2/77 K on ACs.

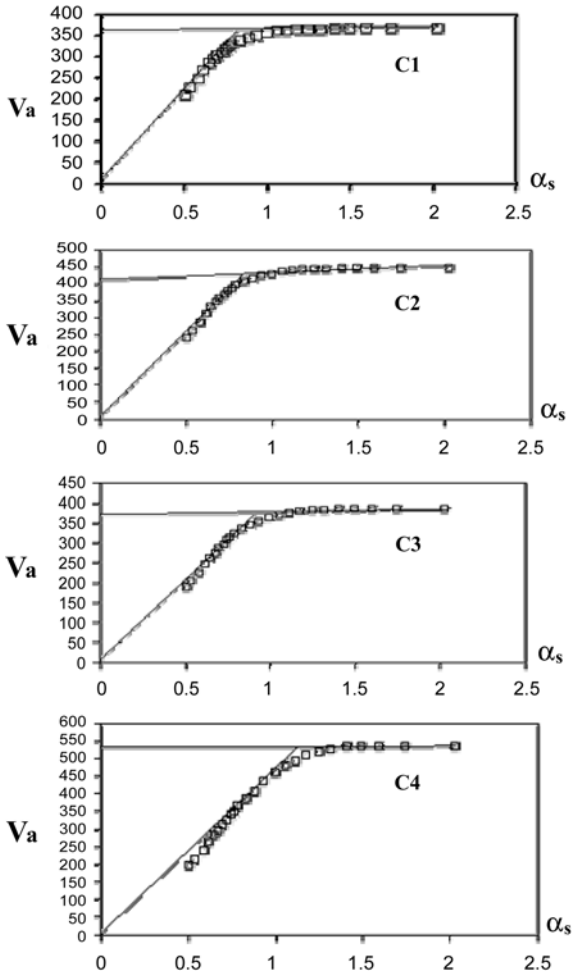

Fig. 2. α_s-Plots of N_2 adsorption on ACs.

Table 1. Porous Properties of Activated Carbons Prepared from Peach Stones at 500 °C

Parameter	C1 30%H_3PO_4	C2 40%H_3PO_4	C3 50%H_3PO_4	C4 70%H_3PO_4
S_{BET} (m^2/g)	1153	1123	1393	1298
V_P (ml/g)	0.5762	0.5960	0.6895	0.8284
Mean radii (r, Å)	10.0	10.6	9.9	12.8
S^{α}_t (m^2/g)	1204	1120	1407	1249
S^{α}_n (m^2/g)	17	33	55	156
V^{α}_o (ml/g)	0.5504	0.5658	0.6339	0.6448
V_{meso} (ml/g)	0.0258	0.0302	0.0556	0.1836
S^{α}_n/ S^{α}_t	0.014	0.029	0.039	0.125
V^{α}_o/V_P	0.955	0.949	0.919	0.778

Inspection of the data in Table 1 reveals that the obtained carbons are highly developed adsorbents with essentially microporous structure (V^{α}_o/V_P = 78-96%, mesoporosity S^{α}_n/ S^{α}_t = 1.4-12.0% and average pore radii = 10-13). However, the surface areas evaluated from the BET- and α_s- methods

are in excellent agreement, and that small irregular variations seem to appear with increased concentration.

The internal pore volume estimates (V_P, V_o, V_{meso}) are enhanced with raised impregnant concentration.

Activation with phosphoric acid (H_3PO_4) has been postulated to affect the precursor and product during the three major stages in the process of the preparation: impregnation (or soaking), pyrolysis and the final leaching of the impregnant [9]. During the course of soaking, the acid introduced into the lingnocellulose produces chemical changes and structural alterations, involving dehydration and redistribution of biopolymers possibly by partial dissolution in the acid solution, together with the cleavage of ether linkages between the lignin and cellulose, followed by recombination reactions in which larger structural units are formed, with the net result of a rigid cross-linked solid. In the pyrolysis stages, the introduced acid dehydrates gradually with continuation of the chemical changes involving cross-linking, water elimination and polymerization. The dehydrated impregnant here reduces tars and volatiles formation, inhibits collapse of the particles, and develops an extensive pore structure, with a consequential increase in the carbon yield. Porosity development in this stage is ascribed to the phosphoric oxides formed at the carbonization temperature, which act as oxidizing agents performing controlled gasification [4]. It may be speculated that higher acid concentrations, or higher impregnation ratios, would enhance porosity development. However, in previous studies [5, 7, 8, 19], it was demonstrated that higher acid concentration were not accompanied by a respective improvement in porosity. Rather, a loss in surface area and pore volume was noticed, which may be attributed to the formation of a layer of polyphosphate (a skin) over the developing pore structure protecting it from an excessive gasification [4].

Finally, the third step in the preparation of an AC, that is the washing and acid recovery, plays a very important role of porosity development. After carbonization, most of the activant is still in the particle and intense washing to eliminate it produces the porosity. It was found by Molina-Sabio *et al.* [11], that there is a good agreement between the volume of micropores and the volume occupied by the acid phase existing at the carbonization temperature. The entrapped polyphosphates in the final product will thus depend on its availability to leaching, and is a function of both impregnation ratio and HTT. The residual entrapped dehydrated acid products will appear in the form of high ash content as well as impart an acidic character on the carbon product (pH ≤ 5.0).

3.2. Liquid-phase Adsorption Characteristics on Activated Carbons

The excellent texture qualities of the four activated carbons obtained by pyrolysis at 500 °C were tested in experiments involving the removal of organic solutes from aqueous solutions. Methylene blue (MB) is one of the most recognized probe molecules and frequently mentioned in the technical specifications of activated carbons [8-10, 20]. In addition, p-nitrophenol (PNP) is a very important and popular probe molecule and represents a model phenolic compound [21-25]. The obtained adsorption isotherms of MB and PNP (Figs. 3 and 4) were analyzed by the linear form of the Langmuir model (eqn. 2) and the estimated equation parameters are shown in Tables 2 and 3. Adopting the well established values 120 and 52.2 Å^2 covered by flat adsorbed MB [26] and PNP [27] molecules, the estimated monolayer capacities (Q_o) were converted into surface area accessible to either MB or PNP (S_{MB} and S_{PNP}). The calculated R_L values are below 1.0 (0.03-0.13) which indicate favorable adsorption.

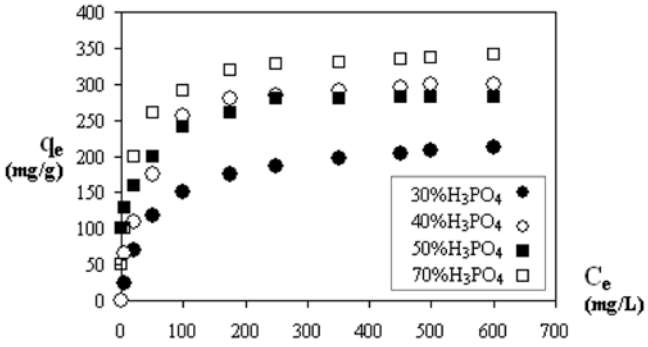

Fig. 3. Adsorption Isotherms of MB from Aqueous Solution on activated carbons.

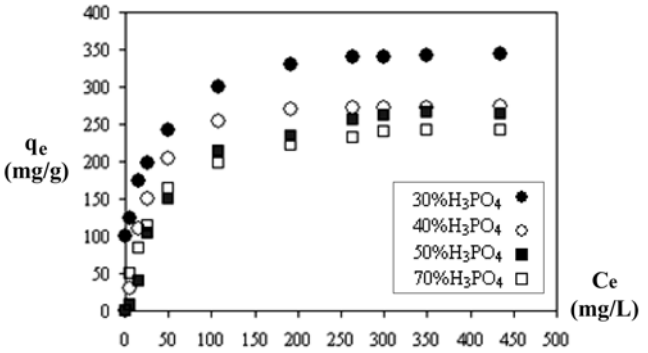

Fig. 4. Adsorption Isotherms of PNP from Aqueous Solution on Activated Carbons.

Methylene blue is adsorbed in a manner determined by the texture characteristics of each adsorbent. An activated carbon prepared by impregnation with 30% H_3PO_4 seems to develop porosity mostly within the narrow microporosity (≤ 10 Å) which is mostly unavailable to the bulky MB molecule. Adsorption of this molecule has been established as suitable for assessing the removal capacity for moderate size pollutant molecules (≥ 15 Å) [28, 29]. Raising impregnant concentration (40-70%) results in developing good porosity, as noticed from S_{BET}, V_P and $V^{\alpha}{}_o$, mostly within

Table 2. Parameters for the Langmuir Isotherms For MB

MB Sorbate / Sample	Q_o mg/g	K_L	ΔG^o KJ/mol	S_{MB} m^2/g	S_{MB}/S_{BET}	SD $\mu.mol/m^2$
C1	198.0	0.032	−23.2	448	0.39	0.5383
C2	309.0	0.032	−23.2	700	0.62	0.8625
C3	362.3	0.046	−24.1	820	0.59	0.8150
C4	411.8	0.017	−21.6	933	0.72	0.9945

Table 3. Parameters for the Langmuir Isotherms For PNP

PNP Sorbate / Sample	Q_o mg/g	K_L	ΔG^o KJ/mol	S_{PNP} m^2/g	S_{PNP}/S_{BET}	SD $\mu.mol/m^2$
C1	344.0	0.027	−20.7	778	0.67	2.146
C2	312.5	0.013	−18.8	708	0.63	2.002
C3	315.8	0.028	−20.8	715	0.51	1.631
C4	337.0	0.017	−19.3	762	0.59	1.868

wide micropores which enhanced considerably the dye removal (310-412 mg/g), and measures areas about 2/3 of the total surface determined by N_2 gas adsorption. It is noticeable that the associated free energies of adsorption (19-24 KJ/mol) indicate that adsorption to be spontaneous (-ve) and of physical nature.

Adsorption of PNP on the four carbons, seems to exhibit almost similar Langmuir parameters (Q_o and K_L) irrespective of the preparation conditions (Q_o = 313-344 mg/g). Although PNP is a smaller probe molecule than MB, yet it covers an identical fraction of the surface (~0.6-0.67) as that of MB. In addition to the screening action of the carbon porosity, we face the competitive adsorption of water onto the acidic surface, thus partially reducing the area available to the PNP molecules [10]. It is well established that activated carbons derived by the H_3PO_4-scheme develop hydrophilic surfaces that favorably adsorb water molecules on the surface pore opening and internal porosity which inhibits the free access of PNP molecules with small effective molecular diameters of about 8 Å. Nevertheless, upon calculating the surface density (SD) of both molecules, expressed as $\mu mol/m^2$, indicates that PNP covers more than double (1.63-2.14 $\mu mol/m^2$) that for MB (0.54-1.00 $\mu mol/m^2$). Such difference would correlate well with the bulkiness factor of the two molecules. Thus, adsorption of PNP under consideration is a function of the two important adsorbent characteristics; texture and the surface chemistry. The latter factor was recently studied [21-25], and arrived to a conclusion that the presence of surface acidic groups suppresses the adsorption of PNP, whereas the presence of non acidic groups postulated as quinones favour the adsorption of PNP [23]. Hydrophilicity of the H_3PO_4-activated carbon was very recently postulated to be basically imparted by the formation of organic phosphorous compounds (e.g., polyphosphates, phosphonic, and phosphonous), as well as phosphines [30, 31]. Oxygen–containing surface groups of acid character (carboxylic, phenolic) should not be ruled out as possible contributors to the acidic properties.

3.3. Sorption Dynamics

Although the present carbons show a high capacity of dye uptake, yet practical applications are conducted under different conditions. Large volumes of low dye loadings are usually treated, and low contact periods are desirably required. One carbon (C4) with highest equilibrium adsorption was tested using one gram with one liter of MB solution either at 75 or 150 mg/L concentrations. Typical concentration- time profiles are shown in Fig. 5. Many kinetic models of adsorption were applied:

a) The simple pseudo first -order, Lagergren equation, in its linear form [32];

$$\log (q_e - q_t) = \log q_e - K_1 \cdot t / 2.303 \quad (5)$$

where q_e and q_t are the amounts of dye adsorbed at equilibrium (mg/g) and at time t (min) respectively, and K_1 is the rate constant of adsorption (L/min).

b) The pseudo second-order equation, based on equilibrium adsorption, may be expressed in its linear form [33],

$$t / q_t = 1 / K_2 \cdot q_e^2 + \frac{1}{q_e} \cdot t \quad (6)$$

It is noted that K_2 and q_e in equation (6) can be obtained from the plot of t / q_t vs. t and there is no need to know any parameter beforehand.

c) The intra-particle diffusion rate constant (K_P) is also obtained by linearization of the curve of expression; $q_t = K_P t^{1/2}$ [34].

The adsorption of MB as function of time (Fig. 5), shows that the dye is removed fastly in the beginning and then more slowly until the equilibrium. This was caused by strong affinity between the dye molecules and the AC, fast diffusion to the external (or accessible) surface was followed by slow pore diffusion into the intraparticle matrix to attain equilibrium [20].

The applicability of the models is checked by constructing

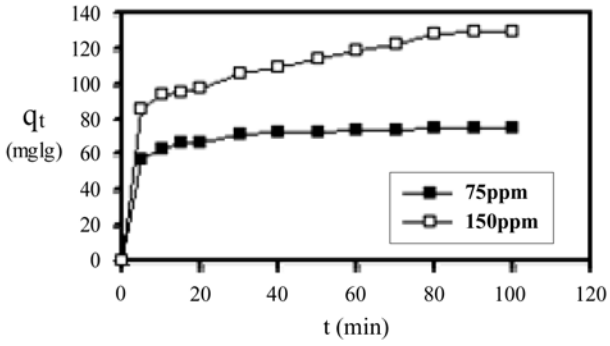

Fig. 5. Kinetic adsorption isotherms of MB on C4.

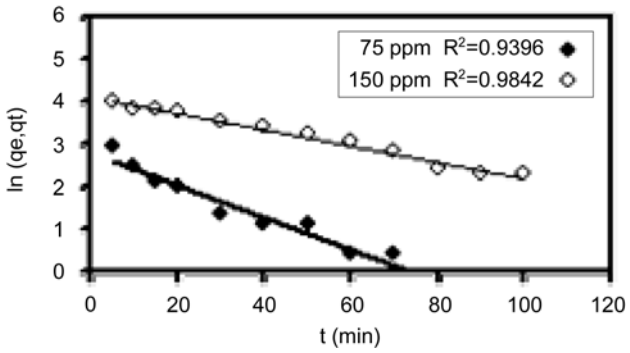

Fig. 6. Linear plot of pseudo-first order kinetics.

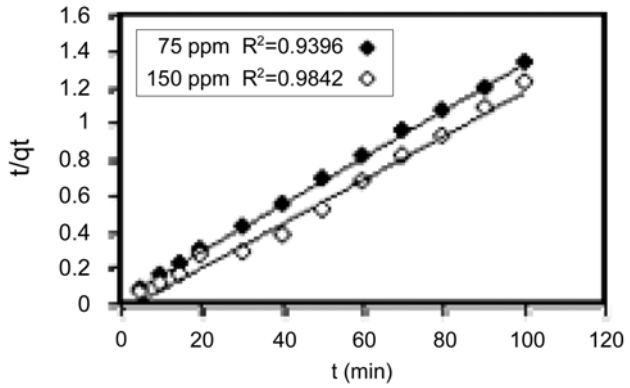

Fig. 7. Linear plot of pseudo-second order kinetics.

the linear plots of ln (q_e–q_t) vs. t, t / q_t vs. t and q_t vs. $t^{1/2}$ as shown in (Figs. 6-8). According to the plots in Fig. 6, the first order plots indicate unsatisfactory correlation coefficients and the calculated q_e values do not agree with the experimental ones (Table 4). This indicates that the adsorption of the dye MB on the AC derived from peach stones is not a first order process. Linear plots in Fig. 7 indicate the applicability of the pseudo-second order equation, with good correlation coefficients (R^2) and q_e values identical to the experimentally determined ones (Table 4). Here, the rate constant of adsorption decreases one order of magnitude by an increase in the initial concentration. The intraparticle diffusion plots (Fig. 8), exhibit multilinearity, indicating that two (or more) steps take place [34]. The first, shaper portion is the instantaneous adsorption stage or external surface adsorption. The second portion is the gradual adsorption

Table 4. Kinetic Parameters for Adsorption of MB on C4

Sample	C_o ppm	Pseudo-1St-order		Pseudo-2nd-order		Intra-particle diffusion
		$K_1 \times 10^{-2}$	q_e	K_2	q_e	K_P
C4	75	4.2	18.2	8.6×10^{-3}	76	3.3
	150	2.1	54.6	9.2×10^{-4}	147	6.1

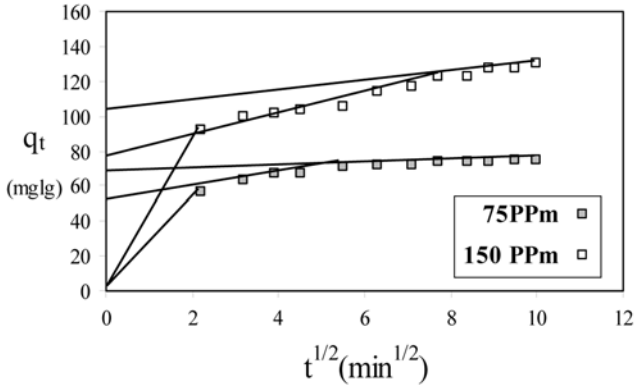

Fig. 8. Intra-particle Diffusion Plot of Adsorption of MB on C4.

stage, where intraparticle diffusion is rate limiting. The third portion is the final equilibrium stage where intraparticle diffusion starts to slow down due to the extremely low adsorbate concentrations left in the solution.

Thus, at limit concentrations of 75 and 150 ppm of MB, the tested high surface area carbon (C4) removed the dye completely within two hours of contact, indicating its high affinity and capacity, and that its internal porosity forms no considerable resistance against free diffusion.

4. Conclusions

Activation of peach stone shells by H_3PO_4 acid resulted in highly developed porosity with high surface area and pore volumes. Increased impregnant concentration at and beyond 50% enhances mostly the internal porosity displayed in the total and micropore volumes, where the latter constitutes more than 80%. Removal capacity towards methylene blue (MB) and p-nitrophenol (PNP), evaluated from equilibrium isotherm data, showed high affinity and capacity. MB is adsorbed in high amounts that cover about 2/3 of the total surface area which regularly increases with acid concentration. Removal of PNP, a smaller ionizable molecule, is high but the amounts uptaken are almost similar irrespective of the different characteristics. PNP seems to be accessible only to less than 2/3 of internal porosity. This might be attributed to the competing adsorption of water molecules on pore openings and internal walls that limit the sites available to PNP. Kinetic adsorption of MB was fast and complete in 2 h at initial concentrations of 75 and 150 ppm, and governed satisfactorily by the pseudo-second-order kinetic law. The initial intra-particle diffusion was a function of initial dye concentration.

References

[1] Manocha, S. *Sādhana* **2003**, *28* (1, 2), 335.

[2] Bansal, R. C.; Donnet, J. B.; Stoeckli, F. "*Active Carbon*", Marcel Dekker, New York, 1988, 4.
[3] Heschel, W.; Klose, E. *Fuel* **1995**, *74*(12), 1786.
[4] Laine, J.; Calafat, A. *Carbon* **1991**, *29*, 949.
[5] Philip, C. A.; Girgis, B. S. *J. Chem. Technol. Biotechnol.* **1996**, *67*, 248.
[6] Girgis, B. S.; Ishak, M. F. *Mater. Lett*. **1999**, *39*, 107.
[7] Khalil, L. B.; Girgis, B. S.; Tawfik, T. A. M. *Adsorpt. Sci. Technol.* **2000**, *18*, 373.
[8] Girgis, B. S.; Yunis, S. S.; Soliman, A. M. *Mater. Lett.* **2002**, *57*, 2002.
[9] Girgis, B. S.; El-Hendawy, A. N. A. *Micropor. Mesopor. Mats.* **2002**, *52*, 105.
[10] Attia, A. A.; Girgis, B. S.; Khader, S. A. *J. Chem. Technol. Biotechnol.* **2003**, *78*, 611.
[11] Molina-Sabio, M.; Rodriguez-Reinōso, F.; Caturla, F.; Selles, M. J. *Carbon* **1995**, *35*, 1105.
[12] Jagtoyen, M.; Derbyshire, F. *Carbon* **1998**, *36*, 1085.
[13] Toles, C. A.; Marshall, W. E.; Johns, M. M. *Carbon* **1997**, *35*, 1407.
[14] Selles-Perez, M. J.; Martin-Martinez, J. M. *J. Chem. Soc. Faraday Trans.* **1991**, *87*, 1237.
[15] Hsieh, G. T.; Teng, H. *J. Chem. Technol. Biotechnol.* **2000**, *75*, 1060.
[16] Kobya, M. *Adsorpt. Sci. Technol.* **2004**, *22*(1), 51.
[17] Rao, M.; Parwate, A. V.; Bohle, A. G. *Waste Manage.* **2002**, *22*, 821.
[18] Selles-perez, M. J.; Martin-Martinez, J. M. *Fuel*, **1991**, *70*, 877.
[19] Castro, J. B.; Bonelli, P. R.; Corella, E. G.; Cukierman, A. L. *Ind. Eng. Chem. Res.* **2000**, *38*, 4166.
[20] Rahman, I. A.; Saad, B. *Malys. J. Chem*. **2003**, *5*(1), 8.
[21] Haghseresht, F.; Lu, G. O.; Whittaker, A. K. *Carbon* **1999**, *37*, 1491.
[22] Chern, J. M.; Chien, Y. W. *Wat. Res*. **2002**, *36*, 647.
[23] Goyal, M. *Carbon Science* **2004**, *5*(2), 55.
[24] Nouri, S.; Haghseresht, F. *Adsorption* **2004**, *10*, 79.
[25] Moreno-Castilla, C. *Carbon* **2004**, *42*, 83.
[26] Giles, C. H.; Trivedi, A. S. *Chem. Ind.* **1969**, 1426.
[27] Daifullah, A. A. M.; Girgis, B. S. *Wat. Res*. **1998**, *32*(4), 1169.
[28] Gergova, K.; Petrov, N.; Minkova, V. A. *J. Chem. Technol. Biotechnol.* **1993**, *56*, 77.
[29] Ahmad, T. W.; Usmani, T. H.; Mumtaz, M. *Pak. J. Sci. Ind. Res*. **1997**, *34*, 121.
[30] Puziy, A. M.; Poddubnaya, O. I. *Mater. Sci. Farum. (Functionally Graded Materials)*, **1999**, *908-913*, pp 308-311.
[31] Puziy, A. M.; Poddubnaya, O. I. Martinez-Alonso, A, Suarez-Garci, F.; Tascon, J. M. D. *Carbon* **2002**, *40*, 1493.
[32] Namasivayam, C.; Kavitha, *Dyes & Pigments* **2002**, *54*, 47.
[33] Tseng, R. L.; Wu, F.-C.; Juang, R.-S. *Carbon* **2003**, *41*, 487.
[34] Inbaraj, B. S; Selvarani, K.; Sulochana, N. *J. Sci. & Ind. Res*. **2002**, *61*, 971.